Scripta Materialia 109 (2015) 94–99

Contents lists available at ScienceDirect

Scripta Materialia

journal homepage: www.elsevier.com/locate/scriptamat

Computational study of $< 1\bar{1}00 >$ symmetric tilt grain boundaries in Mg and Ti

Chang Ni [a,c], Hong Ding [b], Mark Asta [c], Xuejun Jin [a,*]

[a] State Key Lab of Metal Matrix Composites, School of Material Science and Engineering, Shanghai Jiao Tong University, Shanghai 200240, China
[b] Environmental Energy Technologies Division, Lawrence Berkeley National Laboratory, Berkeley, CA 94720, USA
[c] Department of Materials Science and Engineering, University of California at Berkeley, Berkeley, CA 94720, USA

ARTICLE INFO

Article history:
Received 28 April 2015
Revised 19 July 2015
Accepted 21 July 2015
Available online 31 July 2015

Keywords:
Grain boundary energy
Grain boundary structure
Molecular dynamics
Magnesium
Titanium

ABSTRACT

The energetics of $< 1\bar{1}00 >$ symmetric tilt grain boundaries in Magnesium and Titanium was studied based on semiempirical interatomic potential model. For both metals, similar trends of grain boundary energy as a function of tilt angle were observed. Our calculations suggested that the $\{11\bar{2}3\}$ twin boundary is a cusp in the energy versus misorientation plot, and we demonstrated a unique crystallographic reorientation for $\{11\bar{2}6\}$ twin structures. Structure preferences of several twin boundaries were further confirmed with density-functional-theory calculations.

The properties of grain boundaries (GBs) in hexagonal-close-packed (hcp) metals have been widely studied due to their relevance for the mechanical properties of light-weight structural materials such as magnesium (Mg) and titanium (Ti) [1–3]. Symmetric tilt grain boundaries (STGBs) in particular have been the subject of several recent studies [4–6]. Compared with widely-studied cubic crystals, however, STGBs in hcp metals are not as well understood, and several fundamental issues related to the structure and energies of these interfaces continue to be actively investigated.

One topic that has been discussed extensively in the literature is the atomic structure of the $\{11\bar{2}1\}$ twin boundary (TB), which belongs to the set of $< 1\bar{1}00 >$ STGBs in hcp metals. Two distinct structures for this TB have been reported based on atomistic computer simulations, which are referred to as R- and D-configurations [7,8]. The D-configuration is characterized by a different packing sequence of {0001} planes in the two grains across the GB: on one side the stacking is ABAB, while on the other it is ACAC. In the work of Fernández et al. [9], the R-configuration is defined as the configuration with the same packing sequences of basal planes in the two grains (both ABAB), thus displaying mirror symmetry. The asymmetric D-configuration is regarded as the more energetically favored one, relative to the R-configuration, for hcp zirconium (Zr) and Ti [9]. Similarly, the energetic preference for the D-configuration is reported in hcp Zr in a recent atomic simulation [10].

There is some disagreement in the literature concerning the nature of the base structures (BSs) in the $< 1\bar{1}00 >$ STGB family. Generally, BSs correspond to cusps in the energy versus misorientation, and different reports have been made for what values of $\mathbf{x}$ in $\{11\bar{2}\mathbf{x}\}$ twin boundaries (TBs) (where $\mathbf{x}$ ranges from 1 to 6) correspond to BSs. Further, different studies have reached different conclusions about whether asymmetric configurations are more stable than symmetric ones for the differing tilt angles. In very early work, only $\{11\bar{2}1\}$, $\{11\bar{2}2\}$, $\{11\bar{2}3\}$ and $\{11\bar{2}4\}$ TBs are regarded as BSs for nine different hcp metals, and both $\{11\bar{2}1\}$ and $\{11\bar{2}3\}$ TBs are considered asymmetric [11]. By contrast, Farkas studied $\{11\bar{2}\mathbf{x}\}$ TBs in hcp cobalt (Co) and Ti, among which only the structure of the $\{11\bar{2}1\}$ TB is asymmetric [12]. In recent work [13,14], only $\{11\bar{2}1\}$, $\{11\bar{2}2\}$, $\{11\bar{2}4\}$ and $\{11\bar{2}6\}$ TBs are reported as BSs for hcp Mg, Ti and Zr, while $\{11\bar{2}3\}$ and $\{11\bar{2}5\}$ TBs are not. An energy ordering of $\{11\bar{2}1\} < \{11\bar{2}2\} < \{11\bar{2}6\} < \{11\bar{2}4\}$ are suggested for these BSs.

In the present work, molecular dynamics (MD) simulations were employed to extend these previous studies of $< 1\bar{1}00 >$ STGBs in hcp metals, in a study of elemental Mg and Ti. In describing these structures, we extend Fernández's concept of D- and R-configurations to all the $< 1\bar{1}00 >$ STGBs here, considering the

---

* Corresponding author.
E-mail address: jin@sjtu.edu.cn (X. Jin).

http://dx.doi.org/10.1016/j.scriptamat.2015.07.028
1359-6462/

packing sequence of basal planes in the two grains across the GB. We identified a new stable $\{11\bar{2}3\}$ TB structure with D-configuration, and a unique configuration displaying an interesting reorientation of the crystal within the $\{11\bar{2}6\}$ TB. As a result, the energetics of $< 1\bar{1}00 >$ STGBs was revised based on the two configurations uncovered here.

The relaxed structures and GB energies of $< 1\bar{1}00 >$ STGBs were investigated computationally using bi-crystal geometries [13]. The optimization of each GB structure proceeded as follows: (1) An orthogonal system with an hcp structure was built based on $x//[\bar{1}\bar{1}20]$, $y//[1\bar{1}00]$ and $z//[0001]$, as shown in Fig. 1(a). (2) The orthogonal system was rotated $(90 - \theta)$ degrees clockwise and anticlockwise around the tilt axis (y axis) to form two distinct grains. (3) The two new grains were combined together with one shared plane, as shown in Fig. 1(b). Periodic boundary conditions (PBCs) was set along the y and z direction (Fig. 1(c)). The length of simulation cell along the x direction is carefully investigated in order to obtain converged GB energetics (Fig. S2 in Supplementary Materials). (4) Additional shuffles along the y direction were applied to one grain when the initial D-configuration was built, as shown in Fig. 1(b).

The MD simulations were based on two embedded atom method (EAM) potentials for Mg [15,16] and one EAM potential for Ti [17]. In what follows, we refer to the Mg potential due to Liu et al. [15] as Mg-1 and that from Sun et al. [16] as Mg-2. Before minimization and relaxation, a sampling process considering grain shifts and atom removal was carried out to identify energetically stable and metastable configurations. During relaxation, the y and z periodic lengths of the simulation cell evolved dynamically in order to release stress along these directions using a Hoover barostat [18]. MD simulations were performed using the LAMMPS code [19] and the structures were visualized using ATOMEYE [20]. Several GB energies were further computed with density functional theory (DFT) as implemented in the Vienna ab initio simulation package [21,22] using the projector augmented wave (PAW) method [23,24] and Perdew–Burke–Ernzerhof (PBE) exchange–correlation functional [25]. More methodology details related to the sampling process, MD simulations and DFT calculations are presented in Supplemental Material.

Fig. 2(a) plots the GB energies of fully relaxed configurations (including both R- and D-configuration) with respect to the tilt angle θ, calculated with Mg-1. During the relaxation, some of the structures initialized in the R-configuration transformed to the D-configuration, and vice versa. Hence, it should be emphasized that ‘R’ and ‘D’ notations in Fig. 2(a) correspond the final, relaxed states. Transformation between R- and D-configuration is mainly accomplished through $\frac{<1\bar{1}00>}{12}$ atomic shuffle, as discussed further in Supplementary Materials. For every θ, the relatively lower energy between R- and D-configurations is chosen to sketch the corresponding energy envelope of the energy versus misorientation, as shown in Fig. 2(b). These plots can be compared to those presented in previous work [6,13,14]. Results from Mg-2 and Ti potentials are presented in Fig. 2(b) as well. For all three potentials the overall trends in the energy versus θ are similar, except for one significant difference near 23°.

To highlight the overall trends, as well as the behavior near 23°, we split the θ range into seven sets, centered around each of the cusps in the energy plot. Each of these bins is referred to as S-1 to S-7 in what follows. The classification is accomplished according to the following steps: (1) identify the base structures (BSs). The BSs feature higher coherency and lower GB energy than other STGBs with nearby θ, so they represent the cusps in the GB energy versus θ curves [6,13,14]. In the present work, seven BSs are found (named BS-1 to BS-7 in sequence), at $\theta = 0$, 28.41, 39.06, 47.26, 58.36, 72.88 and 90° for Mg-1, respectively. (2) Determine the boundaries between two neighbor sets. This was usually achieved by calculating Burgers Vector of GB dislocation in previous works [13]. In this work, we identify the boundaries through the alternative ordering of the GB energy for R- and D-configurations from

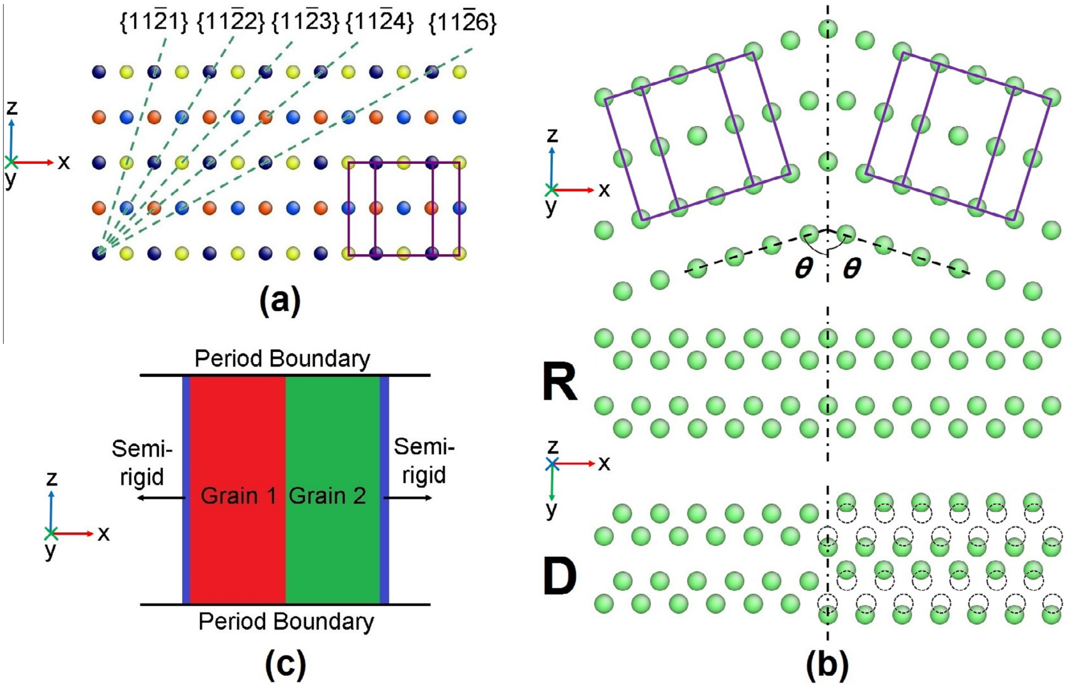

Fig. 1. (a) Initial hcp lattice before rotation. Atoms are colored with the ‘height’ along y direction and green dashed lines represents to the atomic planes. (b) Projections along y and z axis of bi-crystal system. hcp lattice is sketched with purple lines. D-configuration is formed by applying atomic shuffling to R-configuration (open circles for comparison) along y direction. (c) Schematic diagram of boundary conditions of bi-crystal system. PBC is set along y and z direction. Atoms near the surface are semi-rigid. (For interpretation of the references to color in this figure legend, the reader is referred to the web version of this article.)